SYNTHESIS OF PARAFFIN-BASED PHASE CHANGE MATERIAL (PCM) COMPOSITES WITH EXPANDED GRAPHITE AS A COOLING SYSTEM FOR SOLAR PANELS

MUHAMAD FAUZAN AZKA ALFIKRIA[1], SAHRUL HIDAYAT[2], SETIANTO[2]
NOTO SUSANTO GULTOM[2], OTONG NURHILAL[2*]

[1]*Physics Study Program, Universitas Padjadjaran*
[2]*Department of Physics, Universitas Padjadjaran*
Jl. Raya Bandung-Sumedang Km.21 Jatinangor 45363, Sumedang, Jawa Barat, Telp. 022-7796014

*Corresponding author
Email: otong.nurhilal@phys.unpad.ac.id

Abstract. Excessive surface temperatures of solar panels cause electrons in the semiconductors to move very actively. This results in a decrease in output voltage and an increase in internal resistance, reducing the solar panel's ability to effectively convert solar energy into electricity. This problem can be overcome by implementing a cooling system on the solar panel. One such cooling system is a phase change material (PCM). Paraffin is the most commonly used PCM because its melting point is within the operating temperature range of solar panels. However, paraffin has low thermal conductivity. Therefore, paraffin is often composited with materials with high thermal conductivity, such as expanded graphite. Graphite has been expanded using H_2SO_4 and $K_2S_2O_8$ solutions. The results of the expanded graphite test obtained a surface area of 201.95 m²/g. Expanded graphite (EG) is able to increase the thermal conductivity of the PCM composite to 0.31 W/mK, 0.37 W/mK, and 0.44 W/mK with the addition of EG of 5 wt%, 10 wt%, and 15 wt%, respectively. The results of measurements of the surface temperature and efficiency of solar panels with a paraffin wax and expanded graphite composite cooling system show an increase in heat transfer and solar panel efficiency along with increasing the expanded graphite content in the PCM composite. The highest decrease in solar panel surface temperature is 13oC from the surface temperature of the solar panel without PCM and the highest increase in efficiency is 9.7% for the addition of 10% EG to the PCM. The increase in thermal conductivity in the PCM composite has succeeded in transferring heat effectively to the surface of the solar panel.

Keywords: Solar panel; paraffin; expanded graphite; thermal conductivity; efficiency.

Abstrak. *Suhu permukaan panel surya yang berlebihan menyebabkan elektron dalam semikonduktor bergerak sangat aktif. Hal ini mengakibatkan penurunan tegangan keluaran dan peningkatan resistansi internal, sehingga mengurangi kemampuan panel surya untuk secara efektif mengubah energi matahari menjadi listrik. Masalah ini dapat diatasi dengan menerapkan sistem pendingin pada panel surya. Salah satu sistem pendingin tersebut adalah material perubahan fasa (PCM). Parafin adalah PCM yang paling umum digunakan karena titik lelehnya berada dalam kisaran suhu operasi panel surya. Namun, parafin memiliki konduktivitas termal*

yang rendah. Oleh karena itu, parafin sering dikompositkan dengan material dengan konduktivitas termal tinggi, seperti grafit yang diperluas. Grafit telah diperluas menggunakan larutan H_2SO_4 dan $K_2S_2O_8$. Hasil uji grafit yang diperluas memperoleh luas permukaan sebesar 201,95 m^2/g. Grafit yang diperluas (EG) mampu meningkatkan konduktivitas termal komposit PCM menjadi 0,31 W/mK, 0,37 W/mK, dan 0,44 W/mK dengan penambahan EG masing-masing sebesar 5 wt%, 10 wt%, dan 15 wt%. Hasil pengukuran suhu permukaan dan efisiensi panel surya dengan sistem pendingin komposit lilin parafin dan grafit yang diperluas menunjukkan peningkatan perpindahan panas dan efisiensi panel surya seiring dengan peningkatan kandungan grafit yang diperluas dalam komposit PCM. Penurunan suhu permukaan panel surya tertinggi adalah 13°C dari suhu permukaan panel surya tanpa PCM dan peningkatan efisiensi tertinggi adalah 9,7% untuk penambahan 10% EG ke PCM. Peningkatan konduktivitas termal dalam komposit PCM telah berhasil mentransfer panas secara efektif ke permukaan panel surya.

Kata kunci: *Panel surya; parafin; grafit yang diperluas; konduktivitas termal; efisiensi.*

1. Introduction

Solar panels are semiconductor-based devices capable of converting solar energy into electrical energy through the photovoltaic effect. The amount of electrical energy generated by a solar panel is directly proportional to the intensity of the sunlight it receives. Approximately 20% of the solar spectrum is converted into electricity, while more than 50% is transformed into excess heat [1]. The optimal operating temperature for solar panels is around 25°C [2]. When the surface temperature of the solar panel exceeds this optimal value, its performance declines. Several studies have shown that for each 1°C increase beyond the optimal temperature, the efficiency of a solar panel can decrease by approximately 0.45% [3]. One of the major challenges of conventional solar panels is their low efficiency and thermal management issues. Continuous technological advancements in solar panel design aim to significantly enhance their performance, one of which is through the integration of various cooling systems. An effective cooling technique can help maintain optimal photovoltaic temperatures, thereby improving overall photovoltaic efficiency.

One promising cooling solution is the use of Phase Change Materials (PCMs). PCMs are organic or inorganic compounds capable of absorbing and releasing thermal energy in the form of latent heat during phase transitions at nearly constant temperatures. PCMs can absorb excess heat from the surface of solar panels due to their energy storage capacity. Paraffin is one of the most commonly used PCMs because of its melting point, which aligns with the operational temperature range of solar panels, as well as its good chemical stability.

In the research of A.T. Hamada et al. showed that the use of paraffin-based PCM can reduce the average surface temperature of solar panels by about 5°C and increase the average thermal efficiency by 66% [4]. Similarly, Qiu et al. used microencapsulated paraffin-based PCM (MPCM 28), which increased the modified power generation from 10% to 15% [5]. Waqas et al. used paraffin-based PCM (RT24) encapsulated in copper pipes, resulting in a surface temperature reduction of 6°C and an increase in electrical efficiency of 3% [6]. Elsabahy et al. used aluminum-encapsulated paraffin-based PCM (RT25 and RT35), achieving a total electrical efficiency increase of 21.3% and a thermal efficiency increase of 5.3% [7]. Furthermore, Su et al. combined paraffin-based PCM with solar analysis, increasing the total electrical efficiency by 10% and the thermal efficiency by 5% [8].

Paraffin has a very low thermal conductivity value, around 0.2 W/m·K, making paraffin a poor heat conductor due to its ability to absorb and release heat slowly, making it less effective when used as a solar panel cooler. To increase the conductivity of PCM, paraffin must be combined with materials that have high thermal conductivity, such as graphite. Graphite offers a large surface area and excellent thermal conductivity, which can improve heat transfer from paraffin. In addition to thermal conductivity, a large surface area of graphite is required to function as a matrix or 'container' to hold liquid or solid paraffin, prevent it from flowing, and allow for gradual or even release of material. To meet these needs, graphite expansion is necessary to obtain graphite with a large surface area.

Research conducted by Rovida et al. showed that the application of a paraffin-graphite PCM layer to solar panels can reduce the surface temperature by 0.15%, while increasing the efficiency and output power by 19.50% and 0.03%, respectively [9]. Jesus D'Oliveira et al. reported that the addition of expanded graphite (EG) microparticles to a 6 wt% RT62H PCM increased the thermal conductivity to 0.52 W/mK, which was an increase of 156% compared to pure RT62H, which has a thermal conductivity of 0.20 W/mK [10]. Fang et al. studied a composite of paraffin (0.28 W/mK) and EG, using graphite oven-dried at 70°C for 12 hours. Their results showed that increasing the EG content significantly increased the thermal conductivity of the PCM. Among the five variations tested (0.5 wt% to 4 wt%), the 4 wt% EG sample achieved the best result with a conductivity of 2.3 W/mK, which was an increase of 644% [11].

Based on the ability of paraffin PCM combined with expanded graphite to transfer latent heat, this study will be carried out to manufacture paraffin PCM combined with expanded graphite for application as a solar panel cooler. Some important parameters expected are high thermal conductivity of paraffin PCM, large surface area of expanded graphite and optimal electrical efficiency of solar panels with cooling.

2.   Research Methods

The research procedure is divided into several stages, including the preparation of expanded graphite, synthesis of paraffin-based PCM composites with expanded graphite, and experimental measurements of solar panel efficiency.

2.1 Expanded Graphite (EG) Preparation

The graphite powder was expanded using a oxidation agents involving a mixture of sulfuric acid (H_2SO_4) and potassium persulfate ($K_2S_2O_8$). The mass ratio of graphite powder to potassium persulfate was maintained at 1:1. Sulfuric acid solutions were prepared according to the targeted $K_2S_2O_8$– H_2SO_4 ratios: 5%:95% (EG1) and 10%:90% (EG2). The mixture was stirred using a magnetic stirrer at 600 rpm for 60 minutes at room temperature. Following the stirring process, the samples were placed in a water bath at 70°C for 5 minutes. The samples were then filtered using a vacuum filtration system and rinsed with ultra-pure water. Finally, the filtered samples were dried in an oven at 120°C for 12 hours.

2.2 PCM Composite Synthesis

The synthesis process of the PCM composites involved blending expanded graphite with paraffin. Paraffin wax and expanded graphite were weighed according to the desired composition. The paraffin was melted at approximately 120°C using a hot plate. Once

melted, the paraffin was stirred with a magnetic stirrer to ensure complete liquefaction. Expanded graphite was then gradually added to the molten paraffin and stirred continuously for 30 minutes at 1000 rpm. Four composite variations were prepared with different weight percentages of expanded graphite: 0 wt%, 5 wt%, 10 wt%, and 15 wt%. The resulting PCM composites were poured into aluminum molds with dimensions of 19 cm × 13 cm ×1 cm. The composites were left at room temperature to solidify.

2.3 Characterization of Materials

The specific surface area of graphite before and after the expansion process was analyzed using the BET (Brunauer–Emmett–Teller) method at the Tekmira Laboratory, Bandung. The surface morphology of the graphite before and after expansion was examined using Scanning Electron Microscopy (SEM) at 100 nm resolution and 30,000× magnification. Additionally, SEM analysis was performed to observe the morphology of the PCM composite materials. Both SEM characterizations were conducted at the Materials Laboratory, National Taiwan University of Science and Technology (NTUST), Taiwan. Thermal conductivity was measured at the Physics Laboratory of Padjadjaran University, Indonesia.

2.4 Solar Panel Efficiency Measurement

The solar panel efficiency measurements were conducted using a solar simulator with a halogen lamp as the light source. This experiment was carried out at the Instrumentation Physics Laboratory, Padjadjaran University. Data collection involved recording the surface temperature, current, voltage, and light irradiation of the solar panel at 5-minute intervals over a period of 3 hours.

(a)   (b)

Figure 1. (a) PCM position behind the solar panel, (b) solar simulator

3. Result and Discussion

The results of the specific surface area test of graphite and EG with the N_2 isotherm method (Brunauer-Emmet-Teller) BET are shown in Table 1.

Table 1. Specific Surface Area of Graphite and EG

Sample	S_{BET} (m^2/g)
Graphite	7.95
EG1	15.67
EG2	201.95

In the oxidation process, $K_2S_2O_8$ acts as an edge-opening agent for graphite and promotes the intercalation of sulfuric acid into the graphite layer, causing decomposition and gas

release, resulting in rapid graphite expansion [12]. Increasing the $K_2S_2O_8$ concentration leads to a more intense oxidation reaction in graphite [13]. Stronger oxidation results in more oxygen-containing functional groups (such as epoxy, hydroxyl, carbonyl, and carboxyl) in the graphite layer. These functional groups weaken the Van der Waals forces between the layers, thus facilitating the exfoliation process [14]. H_2SO_4 helps stabilize the oxidized structure through capillary action and electrostatic interactions between solution ions and the graphite layer [15].
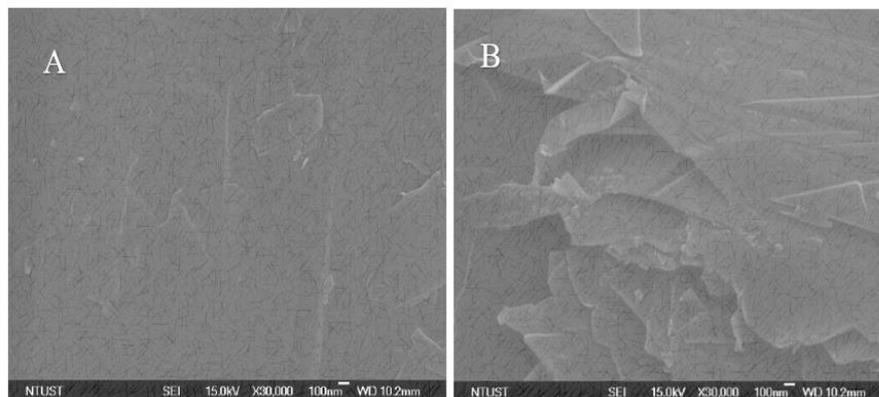

Figure 2. SEM of (A) Graphite (B) Expanded Graphite

Figure 2(A) shows the typical layered structure of graphite. These layers appear thin and flat, indicating that graphite has a lamellar structure with weak van der Waals forces between the layers. This observation is consistent with the anisotropic nature of graphite, where strong covalent bonds exist within the layers (in-plane), while the interactions between the layers (out-of-plane) are relatively weak [16]. The surface morphology appears smooth and uniform, with only small cracks visible between the layers.

In contrast, Figure 2(B) shows exfoliated and expanded graphite layers with visible gaps and separation. The expansion process successfully separated the graphite layers due to the release of gases (such as SO_2 or O_2) during the heating stage after intercalation with sulfuric acid (H_2SO_4) and potassium persulfate ($K_2S_2O_8$). This result indicates that the graphite lamellar structure has undergone a significant increase in surface area. The appearance of gaps, pores, and cavities between the previously dense layers indicates successful exfoliation. This exfoliated structure contributes to a significant increase in specific surface area, consistent with previous measurements where the surface area increases dramatically [17].

Morphological changes at the microstructural level can affect the mechanical and thermal properties of the material [18]. The more open structure and separated layers result in a substantial increase in surface area, corroborating previous measurements where expanded graphite exhibited a surface area of up to 201.95 m²/g at a 10% solid-to-liquid ratio. Next, EG2 was taken to make PCM composites. The results of thermal conductivity measurements are shown in Table 2.

Table 2. Thermal Conductivity of Graphite and Expanded Graphite

Sample	Thermal Conductivity (W/mK)
Graphite	151.42
EG2	244.72

The measured thermal conductivity of graphite is 151.42 W/mK, which is within the typical range for graphite, indicating that the measurement is quite accurate. Pure graphite can exhibit in-plane thermal conductivity values up to 400 W/mK, while graphite with structural defects or contamination generally exhibits lower values, typically in the range of 200 W/mK, depending on the degree of structural disorder [19]. In EG2, the expansion process increases the effective surface area and can optimize heat transfer paths. Although expansion increases the interlayer spacing, it can also improve the alignment of the graphene layers, thus facilitating more efficient heat conduction. Despite being more porous, expanded graphite retains high thermal conductivity due to its restructured morphology, which favors more effective phonon transport [20].

The results of the thermal conductivity measurements of PCMs are shown in Figure 3. The first sample consisted of 100% paraffin wax (PW). The measured thermal conductivity was 0.21 W/mK, which is in good agreement with the typical conductivity range of commercial paraffin, approximately 0.2–0.22 W/mK [21]. With the addition of 5 wt% expanded graphite (EG) to form a PW/EG (95%/5%) composite, the thermal conductivity increased to 0.31 W/mK. This increase indicates that even a small amount of expanded graphite begins to form additional conductive paths within the polymer matrix. The layered structure of graphite facilitates thermal transfer through electron and phonon conduction mechanisms. For the PW/EG (90%/10%) sample the thermal conductivity increased to 0.37 W/mK. Increasing the EG content increases the number of conductive paths within the paraffin, thereby improving the heat transfer performance.

In the PW/EG (85%/15%) sample, the thermal conductivity reached 0.44 W/mK. This result indicates a nearly linear relationship between the amount of graphite added and the increase in the thermal conductivity of the composite. Furthermore, the addition of graphite at this level did not adversely affect the thermal stability of the material.
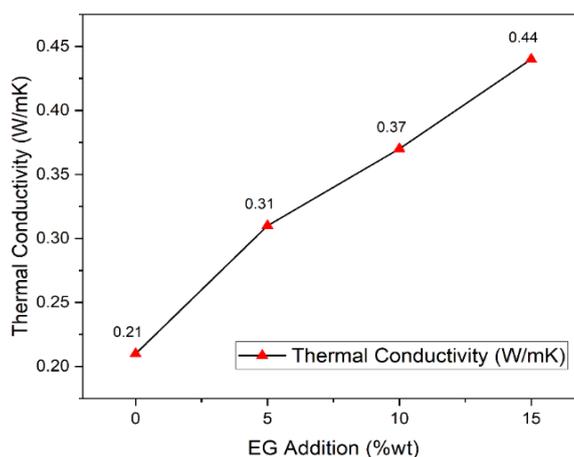

Figure 3. Effect of EG Addition on the Thermal Conductivity of PCM

The increase in thermal conductivity is due to the dispersed expanded graphite particles, which enhance the phonon conduction network and create additional thermal pathways between particles [22]. The SEM test results for PCM are shown in Figure 4.
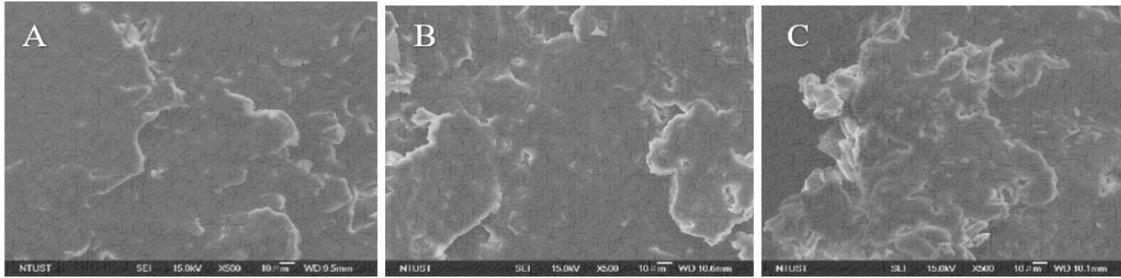
Figure 4. SEM Characterization Results of PCM Composites: (A) PW (100%) (B) PW/EG (95%/5%) (C) PW/EG (90%/10%)

In the PW sample, as shown in Figure 4(A), the surface structure appears relatively dense and smooth. The particles are homogeneously distributed, showing minimal flaking or cracking. This morphology reflects the dominant presence of pure paraffin wax (PW) without significant structural influence from EG. The inherent smoothness of the PW surface is consistent with this observation. The brighter regions in the image correspond to areas with rougher or higher topography, where backscattered electrons are more concentrated, resulting in increased brightness [23].

In the PW/GE (95%/5%) composite, as shown in Figure 4(B), the surface morphology began to show increased porosity and irregularities compared to pure PW. Small cracks were observed, indicating the presence of EG particles within the PW matrix. The addition of small amounts of EG contributed to the formation of micro-voids and pores, potentially enhancing heat transfer pathways. The thermal conductivity increased to 0.31 W/mK, marking an initial increase in heat transfer efficiency due to the addition of EG. Furthermore, the increase in bright regions indicated greater surface roughness and agglomeration. Agglomerates often exhibit a different surface texture compared to well-dispersed regions, and the clumping of EG can lead to areas that appear rougher or denser under SEM [24]. (Hussain et al., 2012).

In the PW/EG (90%/10%) composite, as shown in Figure 4(C), the surface becomes more textured and complex, with greater porosity and a higher visible EG distribution. The increased EG content leads to a more open structure, thus enhancing heat transfer through increased interparticle contact. The thermal conductivity reaches 0.37 W/mK, the highest among the three characterized samples, due to the wider thermal conduction paths formed by the EG network. This sample also exhibits larger bright regions, further indicating increased agglomeration.

Regions exhibiting EG agglomeration contain a higher density of conductive fillers, which can result in non-uniform thermal distribution within the composite. Such non-uniformity can lead to the formation of thermal hot spots or cold zones [25]. In PCM matrices such as paraffin, which are used for latent heat storage applications, this agglomeration can negatively impact heat transfer throughout the matrix, potentially slowing or reducing the efficiency of energy storage and release [26]. The results of PCM testing on solar panels are shown in Figure 5.
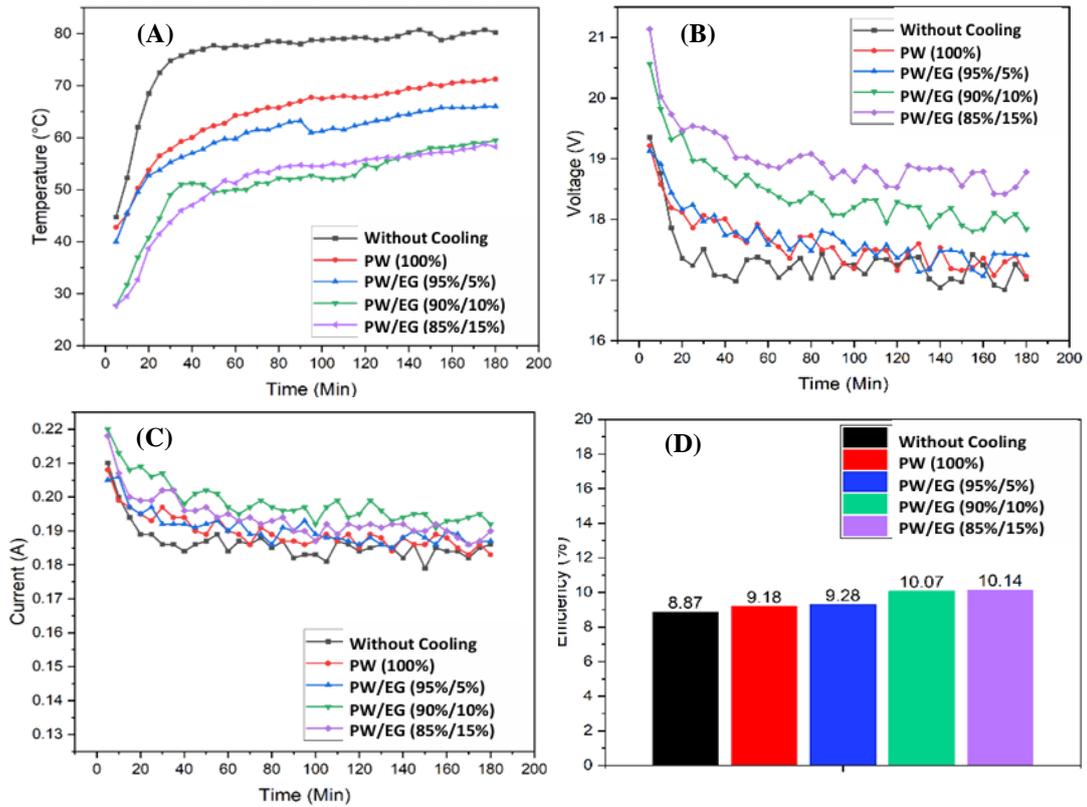
Figure 5. Graphs of (A) Temperature vs. Time (B) Voltage vs. Time (C) Current vs. Time (D) Solar Panel Efficiencies

From Figure 5(A), we can observe the surface temperature graph for each experimental variation. The experiment without a cooling system produced the highest surface temperature, reaching 76.2°C. The cooling system using 100% Paraffin wax (PW) produced a slightly lower average surface temperature of 64.34°C, which represents a decrease of 15.36%. The cooling system using a PW/EG composite (95%/5%) had an average surface temperature of 60.11°C, a decrease of 20.32%. The PW/EG composite (90%/10%) showed a further decrease to 51.36°C or 32.44%, while the lowest average surface temperature was achieved using the PW/EG composite (85%/15%), which was 51.29°C, or 32.52% lower. This correlates with the thermal conductivity of the cooling material: the higher the thermal conductivity, the better the heat flow. Thus, this material can absorb and release heat efficiently between the solar panel surface and the phase change material, thereby effectively lowering the surface temperature.

From Figure 5(B), we can see the voltage graph produced for each experiment. The test without a cooling system produced the lowest average voltage, at 31.3V. The 100% paraffin wax system produced a slightly higher average voltage, at 17.61V. The PW/EG (95%/5%) composite produced an average voltage of 17.68V, while the PW/EG (90%/10%) composite produced 18.44V. The highest voltage recorded was 19V for the PW/EG (85%/15%) composite. This indicates that as the surface temperature increases, the solar panel's voltage output decreases. As the panel's surface temperature increases, additional thermal energy disrupts the semiconductor's energy levels, reducing the open-circuit voltage (Voc). The voltage output of a solar panel is closely related to the bandgap energy of the semiconductor material. As temperature increases, the bandgap energy decreases, requiring less energy to separate electrons and holes [27].

Figure 5(D) shows that the efficiency increases by 3.5% from SP to SPPW. The efficiency increases from SPPW to SPPWEG5, SPPWEG10, and SPPWEG15 were 1.1%, 9.7%, and 10.5%, respectively. A 10% increase in EG resulted in a significant increase in efficiency. This is due to the cooling system's ability to lower the solar panel's surface temperature to near its standard operating temperature.

4. Conclutions

The PW/EG composite as a phase change material (PCM) successfully improved the performance of solar panels. The addition of EG effectively increased the thermal conductivity of the PCM from 0.21 W/mK (pure PW) to 0.44 W/mK at 15% EG content, resulting in improved heat dissipation and a decrease in the surface temperature of the solar panels. The lowest surface temperature observed was 51.29°C, representing a 32.52% decrease compared to the uncooled system. This thermal regulation led to an increase in voltage output, with the highest voltage (19 V) obtained from the panel using the 85%/15% PW/EG composite. Although the current output showed minimal variation due to its dependence on light intensity rather than temperature, the overall solar panel efficiency increased with improved thermal management. These findings confirm that the addition of EG into the PCM matrix improves the system's heat transfer capability, resulting in more stable panel operation and improved solar panel performance.

Acknowledgments

References

1. S. Irvine, "Solar Cells and Photovoltaics," in Springer Handbook of Electronic and Photonic Materials. Eds. Boston, MA: Springer US, 2007, pp. 1095–1106. doi: 10.1007/978-0-387-29185- 7_46.
2. Yusuf, P. (2017) Implementasi Water Cooling System untuk Menurunkan Temperature Losses Pada Panel Surya," J. Tek. Elektro Univ. Tanjungpura, vol. 1, no. 2, pp. 3–5.
3. S. C. Bhatia. Solar devices in Advanced Renewable Energy Systems. Ed. Woodhead Publishing India, 2014, pp. 68–93. doi: 10.1016/B978-1- 78242-269-3.50003-6.
4. Hamada, A. T., Sharaf, O. Z., & Orhan, M. F. (2023). A novel photovoltaic/thermal (PV/T) solar collector based on a multi-functional nano-encapsulated phase-change material (nano-ePCM) dispersion. Energy Conversion and Management, 280(October 2022). https://doi.org/10.1016/j.enconman.2023.116797
5. Qiu, Z., Ma, X., Zhao, X., Li, P., & Ali, S. (2016). Experimental investigation of the energy performance of a novel Micro-encapsulated Phase Change Material (MPCM) slurry based PV/T system. Applied Energy, 165, 260–271. https://doi.org/10.1016/J.APENERGY.2015.11.053
6. Waqas, A., Jie, J., & Xu, L. (2017). Thermal behavior of a PV panel integrated with PCM-filled metallic tubes: An experimental study. Journal of Renewable and Sustainable Energy, 9(5), 53504. https://doi.org/10.1063/1.4995022
7. M. M. Elsabahy, M. Ahmed, H. Sekiguchi, and M. Emam. (2022). Performance assessment of a novel integrated concentrator photovoltaic system with encapsulated

phase change materials. Energy Convers. Manag., vol. 266, p. 115854, doi: https://doi.org/10.1016/j.enconman.2022.11 5854.

8. Su, Y., Zhang, Y., & Shu, L. (2018). Experimental study of using phase change material cooling in a solar tracking concentrated photovoltaic-thermal system. Solar Energy, 159, 777–785. https://doi.org/10.1016/J.SOLENER.2017.11.045

9. Rovida Camalia Hartantrie, Ryann Argadiraksa, & I Gede Eka Lesmana. (2022). Pengaruh Penggunaan Lapisan Phase Change Material Parafin Grafit Sebagai Pendingin Terhadap Efisiensi Panel Surya Polycrystalline. Infotekmesin, 13(2), 329–334. https://doi.org/10.35970/infotekmesin.v13i2.1549

10. E. J. D'Oliveira, U. Azimov, S. C. Pereira, K. Lafdi. Effect of particle size on the thermal conductivity of organic phase change materials with expanded graphite., Energy Storage 92 (2024) 112090.

11. Fang, G., Yu, M., Meng, K., Shang, F., & Tan, X. (2020). High-Performance Phase-Change Materials Based on Paraffin and Expanded Graphite for Solar Thermal Energy Storage. Energy & Fuels, 34(8), 10109–10119. https://doi.org/10.1021/acs.energyfuels.0c00955

12. Hou, B., Sun, H., Tong-jiang, P., Zhang, X., & Ren, Y. (2020). Rapid preparation of expanded graphite at low temperature. 35(3). https://doi.org/10.1016/S1872-5805(20)60488-7

13. Xu, Y., Zhao, L., Bai, H., Hong, W., Li, C., & Shi, G. (2014). Chemically converted graphene induced molecular flattening of 2,4,6-trinitrotoluene with enhanced sensitivity and selectivity. ACS Nano, 4(5), 2936–2942. https://doi.org/10.1021/nn100869c.

14. Dreyer, D. R., Park, S., Bielawski, C. W., & Ruoff, R. S. (2010). The chemistry of graphene oxide. Chemical Society Reviews, 39(1), 228–240. https://doi.org/10.1039/b917103g.

15. Park, S., & Ruoff, R. S. (2009). Chemical methods for the production of graphenes. Nature Nanotechnology, 4(4), 217–224. https://doi.org/10.1038/nnano.2009.58.

16. Dresselhaus, M. S., & Dresselhaus, G. (2002). Intercalation compounds of graphite. Advances in Physics, 51(1), 1–186. https://doi.org/10.1080/00018730110113644

17. Shao, Y., Wang, X., Engelhard, M., Wang, C., & Lin, Y. (2010). Facile and controllable electrochemical reduction of graphene oxide and its applications. Journal of Materials Chemistry, 20(4), 743–748. https://doi.org/10.1039/B917975E

18. Eigler, S., Dotzer, C., Hof, F., Bauer, W., & Hirsch, A. (2014). Sulfur species in graphene oxide. Chemistry – A European Journal, 19(29), 9490–9496. https://doi.org/10.1002/chem.201300763

19. Pop, E., Varshney, V., & Roy, A. K. (2012). Thermal properties of graphene: Fundamentals and applications. MRS Bulletin, 37(12), 1273-1281. https://doi.org/10.1557/mrs.2012.203

20. Song, J., Wang, X., & Chang, T. (2014). Enhanced thermal conductivity of expanded graphite/paraffin composite phase change materials for thermal energy storage. Carbon, 77, 490–500. https://doi.org/10.1016/j.carbon.2014.05.043

21. Usman, M., Siddiqui, F., Ehsan, A., Sadaqat, R. A., & Hussain, A. (2020). Improvement of thermal conductivity of paraffin wax, a phase change material with graphite powder. Proceedings of 2020 17th International Bhurban Conference on Applied Sciences and Technology, IBCAST 2020, 16–25. https://doi.org/10.1109/IBCAST47879.2020.9044541

22. Kocaman, M., Akçay, S. B., Güler, O., Çuvalcı, H., & Varol, T. (2024). Effect of

expandable graphite content on the physical, thermal and mechanical properties of novolac matrix composites: Halogen-free flame-retardant polymer composites. Diamond and Related Materials, 150 (November), 111753. https://doi.org/10.1016/j.diamond.2024.111753

23. Goldstein, J. I., Newbury, D. E., Joy, D. C., Lyman, C. E., Echlin, P., Lifshin, E., Sawyer, L., & Michael, J. R. (2018). Scanning electron microscopy and X-ray microanalysis. Springer. https://doi.org/10.1007/978-1-4613-0491-3

24. Hussain, F., Hojjati, M., Okamoto, M., & Gorga, R. E. (2012). Polymer-matrix nanocomposites, processing, manufacturing, and application: An overview. Journal of Composite Materials, 40(17), 1511–1575. https://doi.org/10.1177/0021998306067321

25. Yang, J., Li, D., Zhang, X., Shi, W., & Fang, X. (2016). Enhanced thermal conductivity of polyethylene glycol/expanded graphite phase change materials for thermal energy storage. Carbon, 100, 693–702. https://doi.org/10.1016/j.carbon.2015.12.038

26. Zhang, P., Ma, Z. W., & Wang, R. Z. (2017). An overview of phase change material slurries: MPCS and CHS. Renewable and Sustainable Energy Reviews, 76, 430–450. https://doi.org/10.1016/j.rser.2017.03.049

27. Hagfeldt, A., Cappel, U. B., Boschloo, G., & Sun, L. (2012). Dye-Sensitized Photoelectrochemical Cells. Practical Handbook of Photovoltaics (pp. 477– 542). Elsevier Ltd. http://doi.org/10.1016/B978-0-12-385934-1.00015-5.